

CANCER

Integration of Hedgehog and mutant FLT3 signaling in myeloid leukemia

Yiting Lim,¹ Lukasz Gondek,¹ Li Li,¹ Qiuju Wang,¹ Hayley Ma,¹ Emily Chang,¹ David L. Huso,¹ Sarah Foerster,¹ Luigi Marchionni,¹ Karen McGovern,² David Neil Watkins,³ Craig D. Peacock,⁴ Mark Levis,¹ Bruce Douglas Smith,¹ Akil A. Merchant,⁵ Donald Small,^{1,6} William Matsui^{1*}

FMS-like tyrosine kinase 3 (FLT3) internal tandem duplication (ITD) mutations resulting in constitutive kinase activity are common in acute myeloid leukemia (AML) and carry a poor prognosis. Several agents targeting FLT3 have been developed, but their limited clinical activity suggests that the inhibition of other factors contributing to the malignant phenotype is required. We examined gene expression data sets as well as primary specimens and found that the expression of *GLI2*, a major effector of the Hedgehog (Hh) signaling pathway, was increased in *FLT3*-ITD compared to wild-type *FLT3* AML. To examine the functional role of the Hh pathway, we studied mice in which *Flt3*-ITD expression results in an indolent myeloproliferative state and found that constitutive Hh signaling accelerated the development of AML by enhancing signal transducer and activator of transcription 5 (STAT5) signaling and the proliferation of bone marrow myeloid progenitors. Furthermore, combined FLT3 and Hh pathway inhibition limited leukemic growth in vitro and in vivo, and this approach may serve as a therapeutic strategy for *FLT3*-ITD AML.

INTRODUCTION

Mutations involving internal tandem duplications (ITD) of the FMS-like tyrosine kinase 3 (FLT3) juxtamembrane domain result in constitutive receptor tyrosine kinase (RTK) activity and are clinically associated with high disease burden at diagnosis, short remissions, and poor overall survival (1). *FLT3*-ITD mutations are typically found in acute myeloid leukemia (AML) along with a wide range of other genetic alterations, suggesting that additional cellular events are required for its full pathogenic effects (2, 3). In transgenic mouse models, the expression of *Flt3*-ITD as a single genetic lesion within the hematopoietic system causes a gradual expansion of myeloid cells resembling an indolent myeloproliferative neoplasm (MPN), but other genetic events are required for the full development of AML (4–11). Unfortunately, most of these cooperating genetic lesions cannot be therapeutically targeted, and therefore, the identification of other cellular pathways activated in *FLT3*-mutant cells may lead to improved treatment strategies.

The highly conserved Hedgehog (Hh) signaling pathway is required for normal embryonic development and is active in a wide variety of cancers by promoting tumor cell proliferation and survival (12). Signaling is initiated by binding of one of the three mammalian Hh ligands to the cell surface receptor Patched (PTCH1), a 12-pass transmembrane receptor that inhibits the 7-pass transmembrane protein Smoothened (SMO). After Hh ligand binding, SMO is derepressed and ultimately modulates the three *GLI* transcriptional regulators and expression of target genes such as *CyclinD1* and *N-Myc* to regulate cell proliferation, survival, and differentiation. Although the pathway is silenced in most postnatal tissues, it is reactivated in several solid tumors, and the

clinical activity of the SMO antagonist vismodegib in advanced basal cell carcinoma (abCC) has confirmed that Hh signaling represents a bona fide anticancer target (13).

Aberrant Hh signaling has also been implicated in hematologic malignancies of lymphoid origin, including multiple myeloma and acute lymphoblastic leukemia (14, 15), but its role in myeloid malignancies is less clear. Multiple studies have found that the modulation of Smo activity affects tumor growth in mouse models of BCR-ABL-driven chronic myeloid leukemia (CML) but does not affect the development or propagation of AML induced by the *MLL-AF9* fusion gene (16–18). Because crosstalk between Hh and RTK signaling occurs in several systems (19–21) and because Hh pathway activation accentuates the oncogenic effects of the BCR-ABL tyrosine kinase, we examined the impact of Hh signaling in *FLT3*-ITD AML. We found that the expression of *GLI2* was increased in *FLT3*-ITD compared to wild-type *FLT3* AML cases. Constitutive activation of Hh signaling in the hematopoietic system of mice expressing *Flt3*-ITD enhanced signal transducer and activator of transcription 5 (STAT5) activity, myeloid progenitor expansion, and the development of AML. Furthermore, combined blockade of Hh and FLT3 signaling inhibited leukemic growth in vitro and in vivo. Therefore, aberrant Hh pathway activation promotes the development of AML, and combinatorial therapy with FLT3 and Hh pathway inhibitors may improve the treatment of *FLT3*-mutated disease.

RESULTS

The expression of the Hh pathway effector *GLI2* is increased in *FLT3*-ITD AML

To identify cellular pathways active in *FLT3*-mutant AML, we initially examined several gene expression profiling (GEP) data sets. Early GEP studies distinguished subgroups of AML on the basis of hierarchical clustering, and a landmark report identified two subgroups enriched in *FLT3*-ITD mutations (22). Within one of these *FLT3*-ITD subgroups (cluster 2), the most significantly expressed gene by significance analysis

¹Department of Oncology, Sidney Kimmel Comprehensive Cancer Center, Johns Hopkins University School of Medicine, Baltimore, MD 21287, USA. ²Infinity Pharmaceuticals, Cambridge, MA 02139, USA. ³Cancer Developmental Biology, The Kinghorn Cancer Centre, Garvan Institute of Medical Research, Darlinghurst, New South Wales 2010, Australia. ⁴Taussig Cancer Institute, Cleveland Clinic, Cleveland, OH 44195, USA. ⁵Department of Medicine, Keck School of Medicine, University of Southern California, Los Angeles, CA 90033, USA. ⁶Department of Pediatrics, Johns Hopkins University School of Medicine, Baltimore, MD 21287, USA.

*Corresponding author. E-mail: matsuiw@jhmi.edu

RESEARCH ARTICLE

of microarrays was *GLI2*, a critical effector of Hh signaling required for responsiveness to Hh ligand during embryonic development (23–25). We examined three additional AML data sets and similarly found that *GLI2* expression was higher in *FLT3*-ITD compared to wild-type *FLT3* AML (Fig. 1A) (3, 26, 27). Moreover, within The Cancer Genome Atlas (TCGA), the expression of *GLI2* in *FLT3*-ITD cases correlated with the major Hh target gene *GLI1*, indicative of active Hh signaling (fig. S1A). *GLI2* and its target gene *BCL2* were also overexpressed in primary *FLT3*-ITD clinical specimens compared to both wild-type *FLT3* AML and normal $CD34^+$ hematopoietic stem and progenitor cells (HSPCs) (Fig. 1B), whereas *GLI1* was highly expressed in both *FLT3*-ITD and wild-type AML (fig. S1B). We also examined *FLT3*-ITD specimens within TCGA's data set and found that higher *GLI2* ($P = 0.046$), but not *GLI1* expression, was associated with a shorter median overall survival (fig. S1, C and D). Therefore, the inferior survival of *FLT3*-ITD AML cases overexpressing *GLI2* suggests that the Hh pathway contributes to the pathogenic impact of this common genetic abnormality.

Hh pathway activation drives the progression of indolent myeloproliferative disease

To examine the functional impact of Hh signaling in *FLT3*-ITD AML, we crossed transgenic *Flt3*-ITD mice in which an 18–base pair ITD mutation has been knocked into the *Flt3* juxtamembrane domain with mice expressing the constitutively active SMO mutant, SmoM2, fused to yellow fluorescent protein (YFP) from the *Rosa26* locus (28, 29). Conditional expression of both *FLT3*-ITD and SmoM2 within the he-

matopoietic system was induced by *Mx1*-Cre and poly(I:C) (polyinosinic-polycytidylic acid) treatment and confirmed by polymerase chain reaction (PCR) and the detection of YFP in peripheral blood cells (fig. S2, A to C) (30). Furthermore, we detected the expression of *Gli2* in *Mx1*-Cre;SmoM2 (SmoM2), *Mx1*-Cre;*Flt3*-ITD (Flt3/ITD), and *Mx1*-Cre;SmoM2;*Flt3*-ITD (Flt3/ITD-SmoM2) mice, as well as *Gli1*, a major Hh pathway target, in SmoM2 and Flt3/ITD-SmoM2 mice (fig. S2D). In contrast, *Gli1* and *Gli2* were not expressed in animals lacking *Mx1*-cre. The expression of *Gli2* in the absence of *Gli1* by Flt3/ITD bone marrow cells suggests that *GLI2* does not primarily drive pathway activation but allows cells to be responsive to Hh ligands, similar to what happens in the developing neural tube and genital tubercle (31, 32). We also found that recombinant Sonic Hh (SHH) ligand could induce *Gli1* expression in bone marrow cells of Flt3/ITD but not wild-type mice (fig. S2E).

FLT3-ITD mutations primarily occur in de novo AML and are associated with rapidly proliferating disease, but similar to previous findings, heterozygous *Flt3*-ITD expression in mice resulted in gradually increasing peripheral WBC counts resembling a chronic MPN, with a median life span of 40 weeks; the expression of SmoM2 alone did not alter peripheral blood counts or survival compared to wild-type controls (Fig. 2A) (28). In contrast, the median survival of Flt3/ITD-SmoM2 mice was significantly shorter than Flt3/ITD animals at 12 weeks ($P = 0.0001$) and was associated with elevated peripheral WBC counts and the generation of a new population of $Mac1^+Gr1^{int}$ leukemic blasts about 3 weeks after poly(I:C) administration (Fig. 2, B to D). Within the bone marrow, Flt3/ITD-SmoM2 animals demonstrated significantly increased cellularity compared to Flt3/ITD mice because of the accumulation of an abnormal population of immature $cKit^+Gr1^{int}$ myeloid cells (Fig. 2E; $P = 0.03$). These cells also infiltrated the spleen, resulting in splenomegaly, as well as nonhematopoietic organs such as the liver and lungs (Fig. 2, F and G, fig. S2F, and table S1). Infiltration within the bone marrow also resulted in the reduction of red blood cell and platelet counts (Fig. 2G and fig. S2G). The accelerated death of Flt3/ITD-SmoM2 mice along with increased numbers of myeloid blasts in the bone marrow and spleen, infiltration of myeloid cells into nonhematopoietic organs, and increased number of myeloid cells in the peripheral blood indicate that constitutively active Hh signaling induces disease progression in Flt3/ITD animals to an MPN-like myeloid leukemia based on established criteria (33).

Myeloid progenitor compartments are expanded in Flt3/ITD-SmoM2 mice

Compared to wild-type mice, Flt3/ITD mice display increased numbers of lineage-negative (Lin^-) multipotent bone marrow $cKit^+Sca1^+$ (KSL) HSPCs as well as committed myeloid progenitors (28). In Flt3/ITD-SmoM2 mice, we found that Lin^- cells were increased compared to Flt3/ITD mice, but the frequency and total number of KSL cells, long-term hematopoietic stem cells (KSL $CD150^+CD48^-CD34^-$), short-term hematopoietic stem cells (KSL $CD34^+Flk2^-$), and multipotent progenitors (KSL $CD34^+Flk2^+$) did not change (Fig. 3, A and B, and fig. S3A). In contrast, $cKit^+Sca1^-Lin^-$ myeloid progenitors were increased by two-fold in Flt3/ITD-SmoM2 mice, primarily due to the expansion of granulocyte/monocyte progenitors (GMPs; $cKit^+Sca1^-Lin^-CD34^+Flk2^+$) but not of common myeloid (CMP; $cKit^+Sca1^-Lin^-CD34^-Flk2^-$) or megakaryocyte/erythrocyte progenitors (MEPs; $cKit^+Sca1^-Lin^-CD34^-Flk2^-$). Therefore, peripheral blood leukocytosis and the increased frequency of leukemic blasts in Flt3/ITD-SmoM2 mice arise from the relative expansion of the GMP compartment.

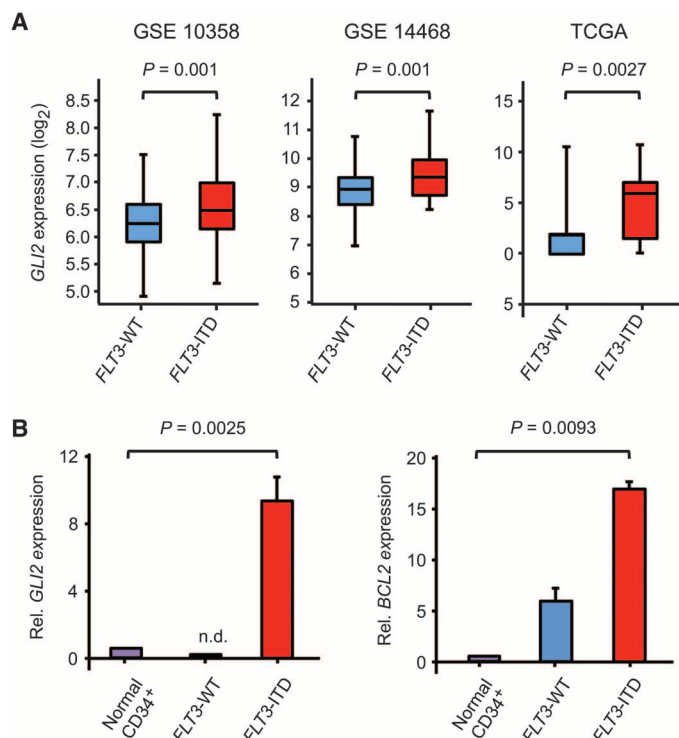


Fig. 1. *GLI2* expression is increased in human *FLT3*-ITD AML. (A) *GLI2* expression in human AML data sets (probe *GLI2* – 228537_at) or TCGA. **(B)** Relative *GLI2* and *BCL2* expression in primary AML samples compared to normal $CD34^+$ HSPCs [$n = 5$ for HSPCs, wild-type (WT) *FLT3*, and *FLT3*-ITD specimens]. Data represent mean \pm SD. n.d., not detected.

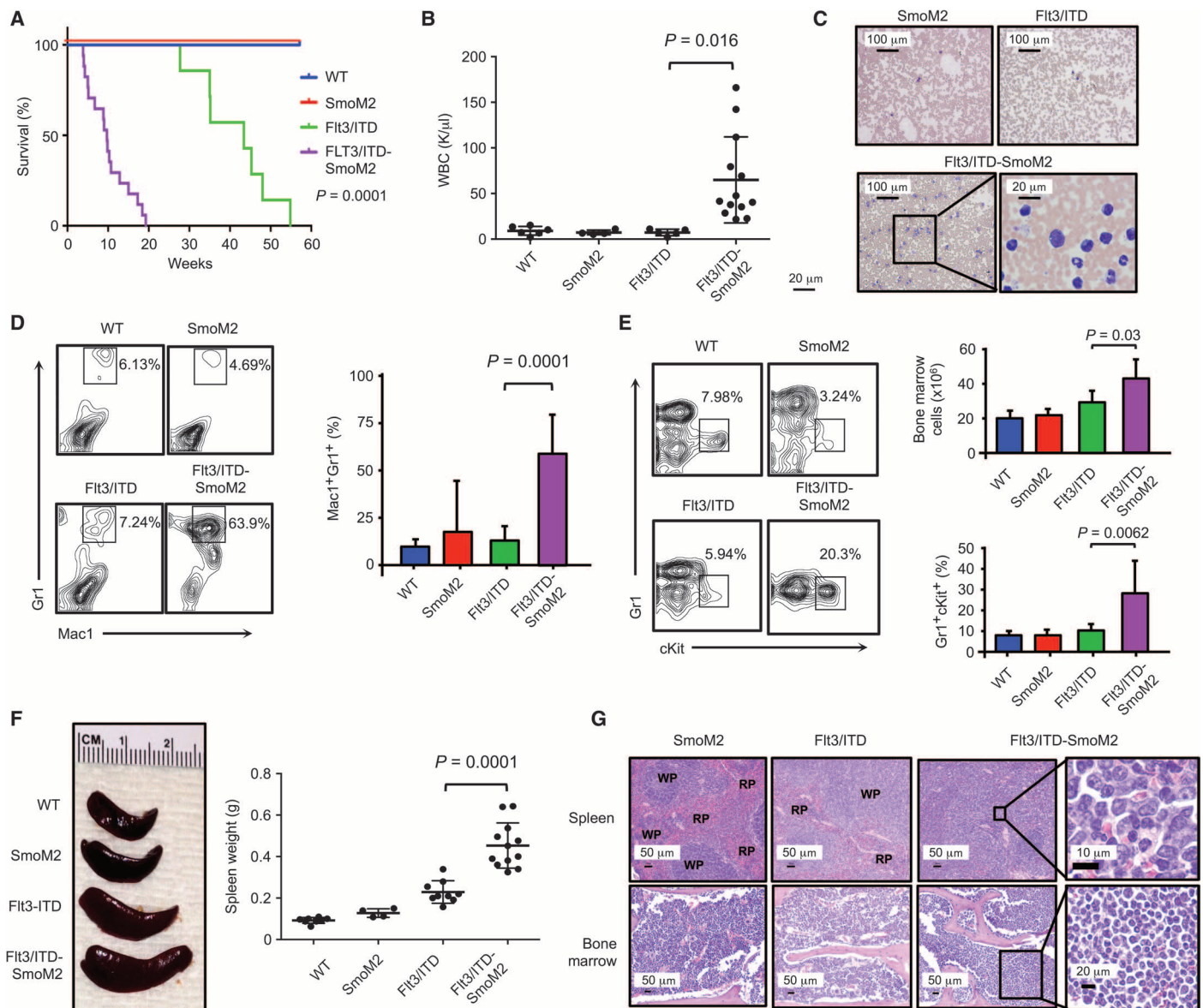


Fig. 2. FIt3/ITD-SmoM2 mice develop rapidly fatal AML. (A) Kaplan-Meier survival curve of transgenic animals after poly(I:C) induction. Statistical significance determined by log-rank (Mantel-Cox) test comparing FIt3/ITD and FIt3/ITD-SmoM2 animals. (B) White blood cell (WBC) counts at 3 months after the completion of poly(I:C) treatment. Data represent mean \pm SD. (C) Wright-Giemsa staining of peripheral blood smears. (D) Fluorescence-activated cell sorting (FACS) analysis of peripheral blood

cells. Bar graph represents percentage of Mac1⁺Gr1⁺ cells ($n = 5$ to 7 per genotype). Data represent mean \pm SD. (E) FACS analysis of bone marrow cells. Bar graph depicts bone marrow cellularity and percentage of Gr1⁺cKit⁺ cells ($n = 3$ to 7 per genotype). Data represent mean \pm SD. (F) Spleen weights and representative spleen sizes. Data represent mean \pm SD. (G) Hematoxylin and eosin staining of bone marrow and spleen sections. RP, red pulp; WP, white pulp.

The proliferation of myeloid progenitors is increased in FIt3/ITD-SmoM2 mice

Both increased FLT3 signaling and Hh pathway activity enhance the proliferation and survival of myeloid leukemia cells (16, 34). To determine the impact of Hh signaling on FLT3-ITD cells, we studied the proliferation of bone marrow cells by quantifying bromodeoxyuridine (BrdU) incorporation. Compared to FIt3/ITD mice, BrdU incorporation in bone marrow cells of FIt3/ITD-SmoM2 mice was similar for most primitive HSPC populations (fig. S3B), but it was increased by greater than twofold in GMPs, which were markedly expanded in the

bone marrow of FIt3/ITD-SmoM2 mice (Fig. 3, C and D). BrdU incorporation was also increased in KSL cells and MEPs, although total numbers of these cells were not increased in FIt3/ITD-SmoM2 mice. Therefore, Hh pathway activity increases the number of GMPs by increasing their proliferative potential.

Hh signaling affects malignant hematopoiesis in a cell-intrinsic manner

In some cancers, aberrant Hh pathway activation is mediated by auto-crine signaling, in which tumor cells both produce and respond to Hh

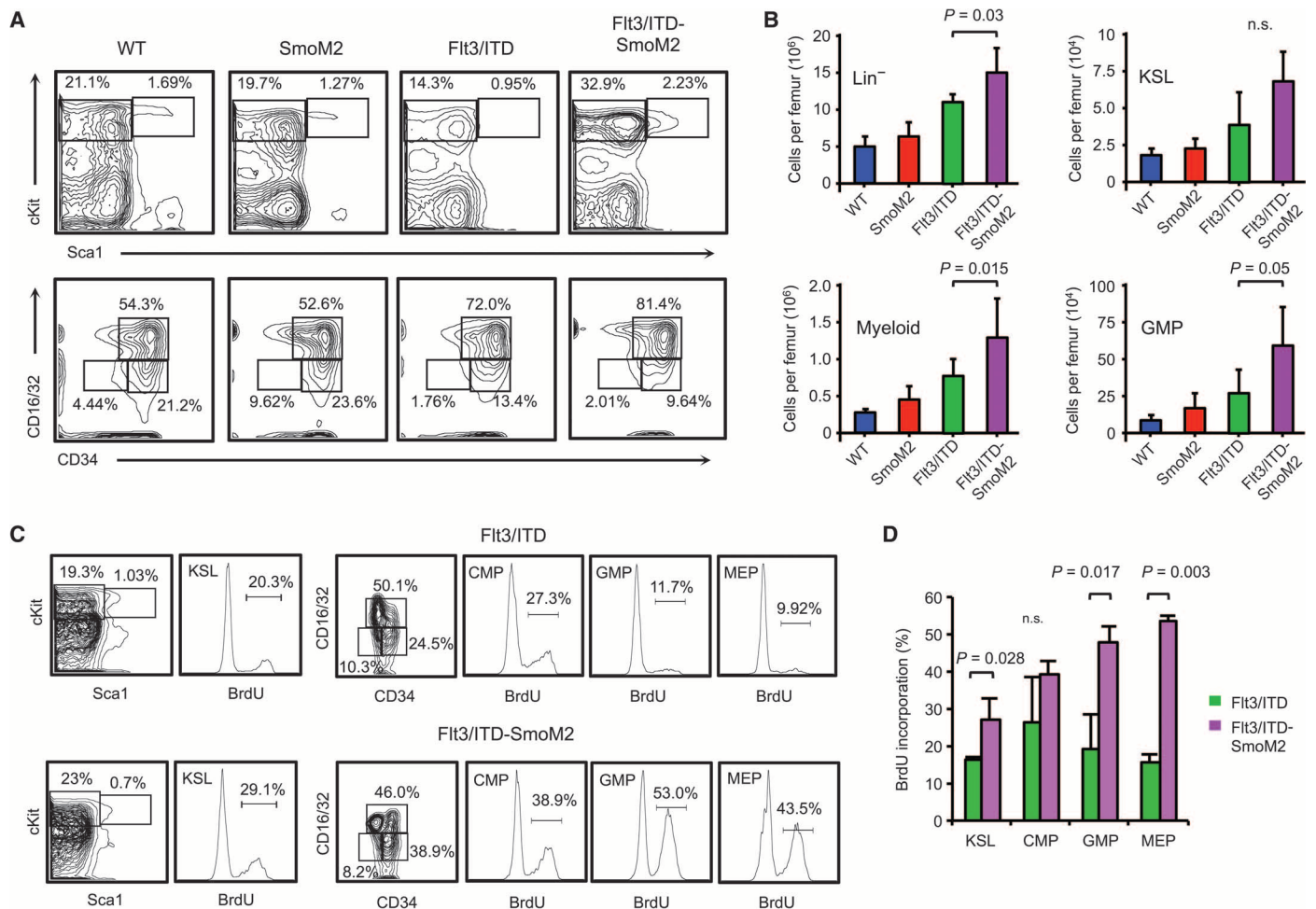


Fig. 3. Myeloid progenitors are expanded and more proliferative in Flt3/ITD-SmoM2 mice. (A) Representative FACS plots depicting relative percentages of stem and progenitor KSL (Lin⁻Sca1⁺cKit⁺), myeloid progenitor (Lin⁻Sca1⁺cKit⁺), GMP (Lin⁻Sca1⁺cKit⁺CD34⁺CD16/32⁺), CMP (Lin⁻Sca1⁺cKit⁺CD34⁺CD16/32⁻), and MEP (Lin⁻Sca1⁻cKit⁺CD34⁺CD16/32⁻)

cells in bone marrow of transgenic animals. (B) Total number of cells of each specific type per femur ($n = 3$ to 7 animals per genotype). Data represent mean \pm SD. n.s., not significant. (C) Representative FACS plots of cells with BrdU incorporation in KSL, CMP, GMP, and MEP compartments. (D) Frequency of BrdU-positive cells from each population ($n = 5$). Data represent mean \pm SD.

ligand (14, 35, 36). In other diseases, paracrine signaling has also been described, such that tumor cells secrete Hh ligands and induce pathway activation in nonmalignant stromal cells but not tumor cells (37). We initially studied the role of bone marrow stromal cells in the propagation of leukemia from Flt3/ITD-SmoM2 mice by transplanting AML cells into wild-type recipients. However, we could not detect leukemic engraftment 8 weeks after transplantation despite cell doses of up to 10 million cells, similar to previous studies with Flt3-ITD mice (38). Because the *Mx1* promoter can be activated by poly(I:C) in multiple cell types, including bone marrow stromal cells (30), we next examined whether the generation of AML by SmoM2 requires cell-intrinsic or cell-extrinsic Hh signaling. We transplanted bone marrow from unexcised CD45.2 Flt3/ITD-SmoM2 mice into wild-type congenic CD45.1 recipient animals (fig. S4A). After the generation of stable donor blood chimerism, recipient mice were treated with poly(I:C) and developed AML with similar tumor cell phenotype and survival as Flt3/ITD-SmoM2 mice (fig. S4, B and C). We also detected YFP expression by flow cytometry within CD45.2⁺ bone marrow hematopoietic

cells but not CD45⁻ cells, indicating that stromal cells did not express SmoM2 (fig. S4D). Therefore, Hh signaling enhances AML progression in Flt3/ITD animals in a cell-autonomous manner.

Constitutive Smo activity enhances STAT5 signaling in Flt3-ITD cells

To determine the mechanisms by which Hh pathway activation affects FLT3-ITD signaling, we initially compared the gene expression profiles of isolated KSL and GMP cells from wild-type, Flt3/ITD, and Flt3/ITD-SmoM2 mice. We used Gene Set Enrichment Analysis (GSEA) and focused on biological pathways frequently activated during oncogenesis, such as proliferation, survival, and self-renewal (39). Among the top GSEA sets, we identified a gene signature consistent with increased STAT5 signaling in Flt3/ITD compared to wild-type animals, as expected from the known role of STAT5 as a major downstream target of FLT3-ITD required for the survival and proliferation of myeloid leukemia cells (Wierenga_STAT5_targets_group2) (fig. S5A). We also used the analysis of functional annotation (AFA) method to further

RESEARCH ARTICLE

confirm the enrichment of STAT5 signaling functional gene sets (40, 41). Compared to *Flt3/ITD* mice, the STAT5 signature was further augmented in cells from *Flt3/ITD-SmoM2* mice (Fig. 4A). To confirm these findings, we quantified the expression of STAT5 target genes and found that several were elevated in GMPs isolated from the bone marrow of *Flt3/ITD-SmoM2* mice compared to *Flt3/ITD* mice (Fig. 4B). STAT5 also enhances cell survival, and we found that an antiapoptotic genetic signature was enriched in *Flt3/ITD-SmoM2* compared to *Flt3/ITD* mice (Anti_apoptosis) (fig. S5B).

The extent of STAT5 activation corresponds to disease acuity, as evidenced by homozygous *Flt3^{ITD/ITD}* mice, which experienced a shorter survival than heterozygous *Flt3-ITD* mice (42, 43). In multiple studies, the transformation of MPN to AML is associated with increased STAT5 signaling driven by loss of the wild-type *Flt3* allele to generate hemizygous *Flt3^{ITD/-}* AML (6–8). We examined both whole bone marrow cells and FACS-isolated GMPs and did not find loss of heterozygosity; both wild-type and ITD mutant *Flt3* genes were detected in *Flt3/ITD-SmoM2* animals (fig. S5C). Therefore, Hh pathway activation in *Flt3/ITD-SmoM2* mice promotes increased STAT5 activity and myeloid cell expansion.

Combined FLT3 and Hh pathway inhibition limits AML growth and proliferation in vitro

FLT3-ITD mutations carry a relatively poor prognosis in adult AML (1), and several small-molecule FLT3 tyrosine kinase inhibitors have undergone clinical testing (44–47). Many of these agents can eliminate

leukemic blasts in the peripheral blood, but the clinical responses are transient because tumor cells persist within the bone marrow (48). Seeing that Hh pathway activation enhanced the proliferative effects of *FLT3-ITD*, we examined whether pathway inhibition could augment the activity of FLT3 antagonists. The MV4-11 and Molm-14 human leukemia cell lines harbor the *FLT3-ITD* mutation (49), and we found that both expressed Hh signaling pathway components as well as Indian Hh ligand by RT-PCR (fig. S6A). We treated cells with the tyrosine kinase inhibitor sorafenib, which has clinical activity against *FLT3-ITD* AML (50), and the SMO antagonist IPI-926 to block Hh signaling (51). IPI-926 decreased *GLI1* and *GLI2* gene expression (fig. S6B) and modestly affected the growth of either cell line as a single agent (Fig. 5A and fig. S6C). However, the antiproliferative effects of sorafenib against MV4-11 and Molm-14 cells were significantly enhanced by IPI-926 (Fig. 5A and fig. S6C; $P = 0.015$ and $P = 0.006$) or knockdown of *GLI2* by small interfering RNA (siRNA) (fig. S6D). These effects were specific for SMO inhibition, because both a second SMO inhibitor, LDE225, and siRNA against *SMO* had similar effects to IPI-926 (fig. S6, E and F). Moreover, further activation of Hh signaling in Molm-14 and MV4-11 cells with recombinant SHH ligand limited the effects of sorafenib (Fig. 5B and fig. S6G). Finally, we also found that this combination was active in clinical *FLT3-ITD* AML bone marrow specimens (Fig. 5C).

Leukemic progression within *Flt3/ITD-SmoM2* mice is associated with the increased proliferation of GMPs (Figs. 3C and 5D); therefore, we examined the combined effects of sorafenib and IPI-926 on cell cycle progression and the survival of MV4-11 cells. Sorafenib induced an increase in G_1 and G_2-M cell cycle arrest compared to vehicle-treated cells, and the addition of IPI-926 further enhanced this effect (Fig. 5D; $P = 0.024$ and $P = 0.034$). Furthermore, this combination inhibited in vitro clonogenic leukemia growth more effectively than did either sorafenib or IPI-926 alone (Fig. 5E and fig. S6H). At the concentrations used, sorafenib induced a modest amount of apoptosis measured by Annexin V binding, but this effect was not significantly increased with the addition of IPI-926 or in wild-type *FLT3* HL60 cells that lack *GLI2* expression (fig. S6, I to K). Therefore, dual FLT3 and SMO inhibition primarily affects AML proliferation.

Because we found that the enhanced proliferation of GMPs in *Flt3/ITD-SmoM2* mice is associated with increased STAT5 activity (Fig. 4A), we studied the effects of sorafenib and IPI-926 on STAT5 activity in MV4-11 cells. Sorafenib alone decreased the phosphorylation of STAT5 (pSTAT5), similar to previous reports (52), and it inhibited *GLI1* and *GLI2* expression (Fig. 5, F and G, and fig. S7A). IPI-926 alone also decreased the ratio of pSTAT5 to total STAT5 as well as decreased the overall expression of total STAT5 (Fig. 5, G and H). Treatment with the combination of sorafenib and IPI-926 further decreased overall pSTAT5 compared to either drug alone because of both lower expression of total STAT5 and a decreased proportion of STAT5 that was phosphorylated (Fig. 5F). SHH increased pSTAT5 and limited the effects of sorafenib but did not affect phosphorylated AKT (pAKT) or phosphorylated extracellular signal-regulated kinase (pERK), which can also be increased by FLT3 signaling (fig. S7B). To further demonstrate that the effects of combined treatment with sorafenib and IPI-926 were primarily mediated by STAT5, we studied BaF3 cells engineered to express *FLT3/ITD* (53). In these cells, interleukin-3 (IL-3) can rescue the effects of FLT3 inhibitors through the induction of STAT5 activation, and we found that it also decreased the effects of sorafenib and IPI-926 on both pSTAT5 and cell growth (fig. S7, C and D). Therefore, the

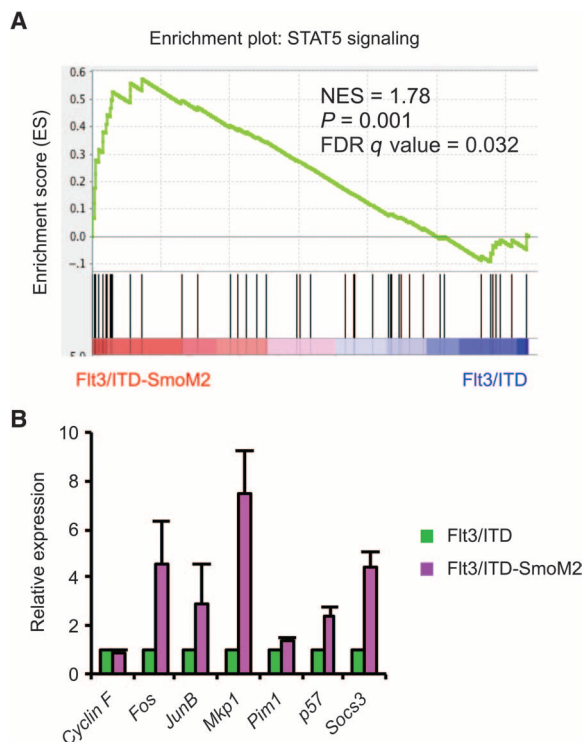


Fig. 4. STAT5 signaling is enhanced in *Flt3/ITD-SmoM2* mice. (A) GSEA analysis comparing *Flt3/ITD* and *Flt3/ITD-SmoM2* mice. NES, normalized enrichment score; FDR, false discovery rate. (B) Quantitative reverse transcription PCR (qRT-PCR) analysis of STAT5 target genes in sorted GMP cells ($n = 3$). Data represent mean \pm SD.

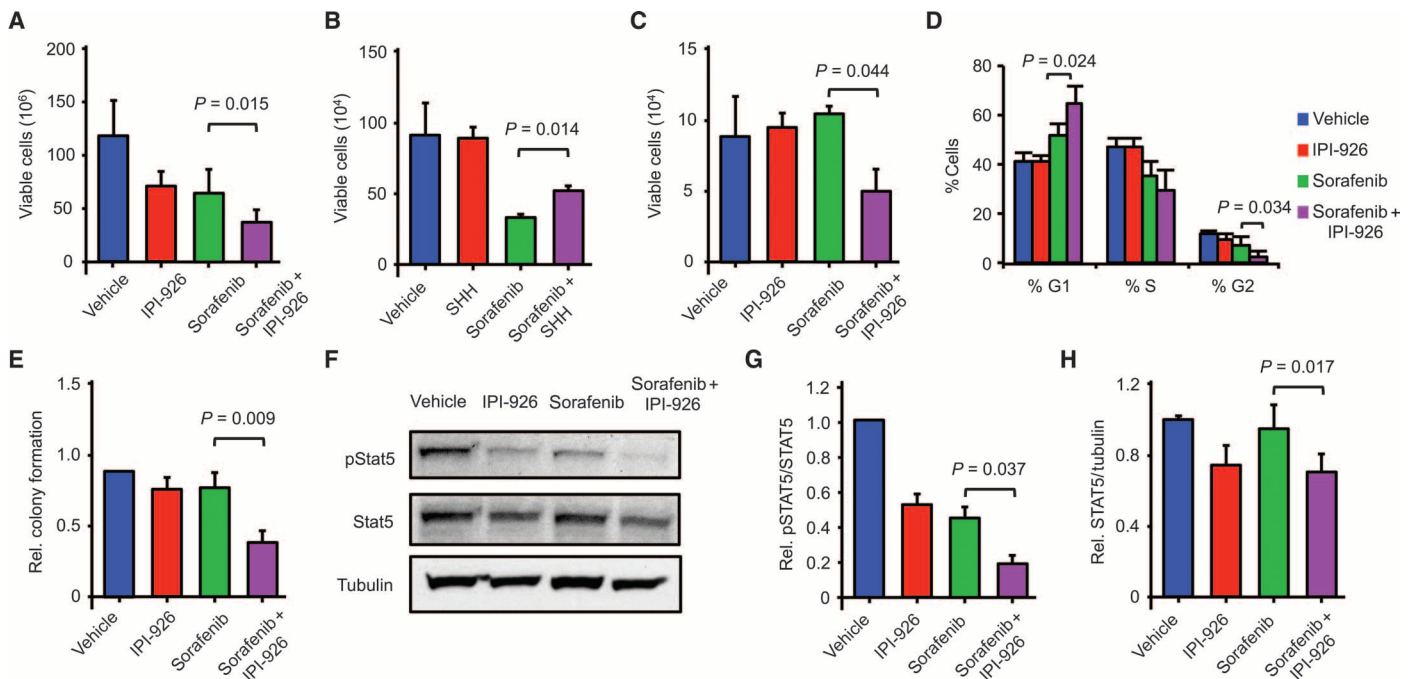


Fig. 5. IPI-926 and sorafenib inhibit leukemic cell growth in vitro. (A) Viable cell counts of MV4-11 cells treated with IPI-926 and sorafenib for 3 days ($n = 4$). Data represent mean \pm SD. (B) Viable cell counts of MV4-11 cell lines treated with recombinant SHH ligand and sorafenib for 3 days ($n = 3$). Data represent mean \pm SD. (C) Viable cell counts of clinical FLT3-ITD AML specimens treated with IPI-926 and sorafenib for 3 days ($n = 4$ individual patients). Data represent mean \pm SD. (D) Cell cycle distribution of MV4-11 cells treated

with IPI-926 and sorafenib after 3 days ($n = 3$). Data represent mean \pm SD. (E) Relative colony formation of MV4-11 cells in methylcellulose after treatment with IPI-926 and sorafenib for 3 days compared to vehicle control ($n = 4$). Data represent mean \pm SD. (F) Western blot of pSTAT5, total STAT5, and tubulin from MV4-11 cells treated for 3 days. (G) Relative ratio of pSTAT5 to total STAT5 ($n = 4$). Data represent mean \pm SD. (H) Relative levels of total STAT5 normalized to tubulin ($n = 4$). Data represent mean \pm SD.

inhibition of the Hh signaling pathway specifically enhances the anti-leukemic effects of FLT3 tyrosine kinase inhibition associated with the inhibition of STAT5.

Sorafenib and IPI-926 cooperate to inhibit leukemic cell growth in vivo

Given the impact of sorafenib and IPI-926 on AML cell lines in vitro, we examined this combination in vivo against *Flt3/ITD-SmoM2*-derived AML. Wild-type recipient mice were engrafted with bone marrow from *Flt3/ITD-SmoM2* mice, treated with poly(I:C), and, after the development of AML, treated with sorafenib and/or IPI-926 daily for 16 days. Although mutated *SmoM2* is relatively resistant to the naturally occurring *Smo* antagonist cyclopamine, IPI-926 inhibits *SmoM2* in vitro and reduced the expression of the Hh target genes *Gli1*, *Gli2*, and *Ptch1* by bone marrow cells in *SmoM2* mice after drug treatment (fig. S8). The combination of sorafenib and IPI-926 reduced splenomegaly compared to either drug alone (Fig. 6A). Furthermore, this combination produced a significant reduction in the percentage of *Mac1*⁺*Gr1*⁺ leukemic cells in the peripheral blood and *Gr1*⁺*cKit*⁺ cells in the bone marrow (Fig. 6B; $P = 0.049$ and $P = 0.045$). Both sorafenib and IPI-926 treatment as single agents increased survival compared to vehicle-treated controls, but the combination further extended survival, with a proportion of the mice failing to succumb to disease despite no further treatment beyond the initial 16-day period (Fig. 6C). Similar to our in vitro studies, treatment with IPI-926 and sorafenib decreased both total STAT5 and active pSTAT5 compared to treatment with sorafenib alone (Fig. 6, D and E).

DISCUSSION

Most newly diagnosed cases of *FLT3*-mutated AML present with rapidly proliferating disease, but *Flt3-ITD* expression in mice causes an MPN marked by the gradual elevation of peripheral WBC counts (28). We found that constitutively active SMO cooperates with aberrant *FLT3* activity to generate AML, and combined treatment with *FLT3* and Hh pathway inhibitors decreased leukemic growth in vitro and in vivo. We also identified increased *GLI2* expression in *FLT3-ITD* clinical AML specimens, suggesting that these findings are clinically relevant. Mutations in Hh pathway components are rare in AML (3), but a recent report also demonstrated that increased wild-type spleen tyrosine kinase (SYK) activity can induce the transformation of *Flt3*-mutant AML (54). Therefore, mutated *FLT3* may remain dependent on the activity of nonmutated cellular pathways for AML pathogenesis.

There are limitations to our study. SMO antagonists are clinically effective in aBCC in which Hh signaling is aberrantly activated by *PTCH1* and *SMO* mutations. We used an *Smo* mutant to constitutively activate the pathway in vivo and found that SMO inhibitors were active when combined with *FLT3* inhibition. However, alterations in *PTCH1* or *SMO* are uncommon in most human cancers, including AML (3, 12), and it is possible that SMO inhibition will not be effective in the absence of these pathway-activating mutations. We also used sorafenib to study *FLT3* inhibition, but several new *FLT3* antagonists, such as quizartinib, are in clinical development (55). Therefore, it is also possible that Hh pathway antagonists will not enhance the activity of these agents because our observed effects were due to the inhibition

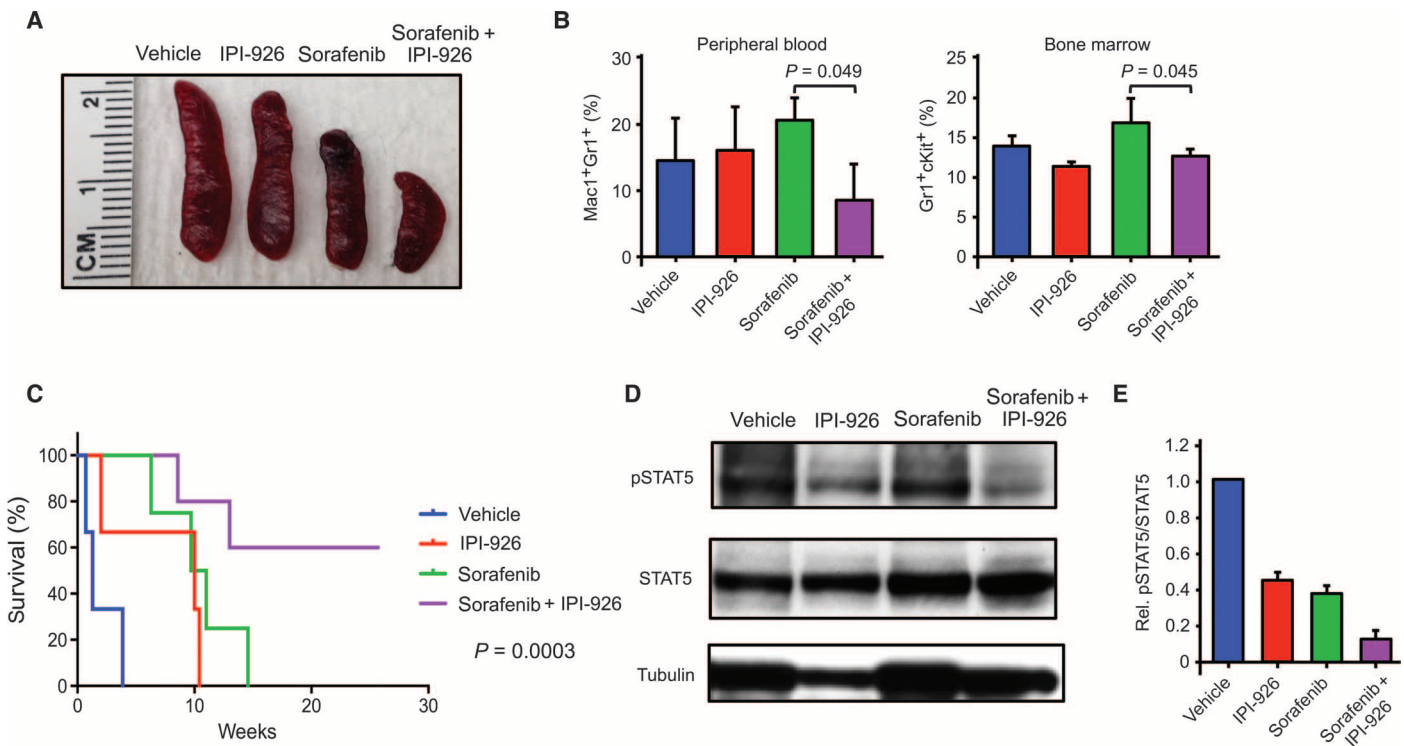


Fig. 6. Combined IPI-926 and sorafenib treatment improves survival. (A) Representative spleen sizes of animals after 16 days of drug treatment. (B) Frequency of abnormal Gr1⁺Mac1⁺ and cKit⁺Gr1⁺ cells in the peripheral blood and bone marrow, respectively, of animals treated with drugs for 16 days ($n = 3$ per group). Data represented as mean \pm SD. (C) Kaplan-Meier

survival curve of animals treated with IPI-926 and sorafenib ($n = 3$ to 5 per group). Statistical significance determined by log-rank (Mantel-Cox) test. (D) pSTAT5 and total STAT5 in bone marrow cells harvested after 24 hours of drug treatment. (E) Ratio of pSTAT5 to total STAT5, normalized to vehicle-treated cells ($n = 3$). Data represent mean \pm SD.

of other kinases that can be targeted by sorafenib (56), and further studies with next-generation FLT3 and Hh pathway inhibitors are needed.

The Hh pathway interacts with several other cellular pathways in a wide range of tumor types (12), and we have identified a functionally relevant interaction between Hh and FLT3 signaling in AML. In several solid tumors, mutant RAS or the activation of RTKs, such as the epidermal growth factor receptor, results in aberrant RAS/RAF/MAPK kinase (MEK) and phosphatidylinositol 3-kinase (PI3K)/AKT signaling and the direct activation of GLI1 (21, 57–59). Although FLT3-ITD is a constitutively active RTK, *Gli1* expression was low in bone marrow cells from *Flt3/ITD* mice at baseline but induced by SHH ligand. In contrast, *Gli1* levels did not change in wild-type cells, and the differential expression of *Gli2* may have restricted Hh ligand responsiveness to *Flt3/ITD* cells. Therefore, *Flt3-ITD* may directly or indirectly induce *Gli2*, which in turn allows canonical signaling by Hh ligand or directly affects AML cell proliferation. Both wild-type and mutant *FLT3* cells expressed more *GLI1* than did normal HSPCs, suggesting that *GLI1* activity may be broadly required in AML. Furthermore, because *GLI2* was primarily increased in *FLT3-ITD* cases and *RAS* mutations are also common in AML (3), *GLI1* activation may broadly occur in AML through Hh ligand-mediated canonical signaling or direct activation by mutant RAS. Sorafenib alone decreased the growth of *FLT3-ITD* cells as well as *GLI1* and *GLI2* expression; therefore, it is also possible that Hh signaling can be at least partially inhibited by FLT3 inhibition alone.

Despite the biologic diversity of mutations that enhance leukemic progression of *Flt3/ITD* mice, a common mechanism for leukemic

progression is the loss of the wild-type *Flt3* allele by acquired segmental uniparental disomy, resulting in increased tyrosine kinase activity and activation of the major downstream target STAT5 (42, 43). Although loss of heterozygosity of the *Flt3* allele did not occur in the *Flt3/ITD-SmoM2* mice, we found that STAT5 activity was increased. STAT5 is one of the main downstream targets of aberrant FLT3-ITD signaling, and increased STAT5 activity is associated with shortened overall survival in patients with *FLT3*-mutated AML (60, 61). The treatment of both human and mouse AML cells with sorafenib and IPI-926 decreased active pSTAT5 by inhibiting both its phosphorylation by FLT3-ITD and total STAT5 expression in response to SMO inhibition. The modulation of STAT5 activity by the Hh signaling pathway has also been described in the development of the mammary gland and brain (62–64), and chromatin immunoprecipitation studies have identified the *STAT5a* gene within GLI1-bound regions in both medulloblastoma and normal granule neuron precursor cells (64). Because STAT5 signaling is important in the pathogenesis of CML as well as other forms of leukemia (65, 66), it is possible that this interaction may also explain the impact of the Hh pathway on BCR-ABL activity (16, 17).

FLT3 mutations are the most common genetic alterations identified in AML, and several inhibitors of FLT3 kinase activity have undergone clinical testing. Although these inhibitors can eliminate leukemic blasts in the peripheral blood, bone marrow responses are much less frequent (48). The failure of these agents to produce complete remissions may be due in part to the lack of in vivo potency and complete and sustained FLT3 inhibition (67). We found that IPI-926 enhanced

RESEARCH ARTICLE

the effects of sorafenib on the proliferation and survival of mutant FLT3 AML cells both in vitro and in vivo. Other recent data demonstrated that inhibition of GLL1 and SMO can enhance the activity of the conventional cytotoxic agent cytarabine in AML, suggesting a broad role for the Hh pathway in therapeutic resistance (68). Therefore, SMO antagonists may improve the clinical utility of FLT3 inhibitors for the treatment of AML through multiple mechanisms.

MATERIALS AND METHODS

Study design

The overall study objective was to determine the role of the Hh signaling pathway in *FLT3*-ITD AML by analyzing the development of leukemia in a transgenic mouse model with or without the constitutive activation of SMO. Sample size calculations were not performed for initial studies, because these were undertaken to identify an interaction between the FLT3 and Hh pathways. Subsequent studies were stopped when double transgenic mice became symptomatic, and littermate controls were analyzed at the same time points. Controlled laboratory experiments also included the analysis of AML cell lines treated with FLT3 and Hh antagonists. Studies were carried out at least in triplicate, and no data were excluded in the final analysis. No blinding occurred throughout the study.

Clinical specimens, cell lines, and drug treatment

Bone marrow specimens were obtained from patients with newly diagnosed AML or normal donors granting informed consent as approved by the Johns Hopkins Medical Institutes Institutional Review Board. CD34⁺ cells were isolated using magnetic microbeads (Miltenyi). Clinical specimens, human *FLT3*-ITD MV4-11 and Molm-14, and wild-type *FLT3* HL60 AML cell lines were cultured in RPMI medium supplemented with 10% fetal bovine serum, 0.5% L-glutamine, and 0.5% penicillin/streptomycin at 37 °C. Similar culture conditions were used for the BaF3/ITD cell line (53). Treatments consisted of IPI-926 (2.5 μM; Infinity Pharmaceuticals), SHH ligand (10 ng/ml; StemRD), LDE225 (5 μM; LC Laboratories), IL-3 (10 ng/ml; PeproTech), and/or sorafenib (LC Laboratories) for 3 days. Sorafenib was used at concentrations of 1 nM for MV4-11 cells and 3 nM for clinical specimens, Molm-14, and BaF3/ITD cells. Viable cells were quantified with a hemocytometer and trypan blue dye exclusion or, in some cases, incubated (500 cells/ml) in methylcellulose at 37 °C for 7 days followed by the quantification of tumor cell colonies (>40 cells per colony) using an inverted microscope (Nikon). Cell viability was also assessed using the Cell Proliferation I Kit (Roche) and an iMark Microplate Reader (Bio-Rad). Cell cycle analysis was carried out by incubating cells in phosphate-buffered saline containing 0.6% NP-40 (Sigma), 40 μg of propidium iodide, and ribonuclease (2 μg/ml) (Roche) followed by flow cytometry analysis with a FACSCalibur (BD Biosciences).

Mice

All animal procedures were approved by the Institutional Animal Care and Use Committee. *Flt3*/ITD mice harboring an ITD mutation knocked into the endogenous *Flt3* locus have been previously described (28). *SmoM2* and *Mx1*-Cre mice were obtained from the Jackson Laboratory. Genotyping was determined by PCR (table S2), and mice harboring alleles heterozygous for *SmoM2*, *Flt3*-ITD, and/or *Mx1*-Cre were obtained. Littermates with single copies of the *SmoM2* or *Flt3*-

ITD alleles were used as controls, whereas wild-type controls carried the *Mx1*-Cre allele alone. After weaning and genotyping, mice were treated with five doses of poly(I:C) (300 μg; Sigma) intraperitoneally every other day, and successful transgene excision was confirmed 4 weeks after the last poly(I:C) injection by PCR of peripheral blood DNA with primers for the loxP sites (table S2). Peripheral blood mononuclear cells were also analyzed for YFP expression by flow cytometry (FACSCalibur, BD Biosciences). The development of AML was assessed by the presence of Mac1⁺Gr1⁺ cells in the peripheral blood and Gr1⁺cKit⁺ cells in the bone marrow by flow cytometry. Mice were sacrificed after the developed lethargy, hunching, and weight loss, and bone marrow was analyzed by flow cytometry. Formalin-fixed tissues were stained with hematoxylin and eosin and blood smears with Wright-Giemsa stain. Complete peripheral blood counts were quantified using a Hemavet 950 analyzer (Drew Scientific).

In vivo drug treatment

IPI-926 was formulated in a 5% β-cyclodextrin (Sigma) solution with deionized H₂O, and mice were given IPI-926 (20 mg/kg) or the same volume of 5% β-cyclodextrin solution once a day for 16 days by oral gavage. Sorafenib was formulated in 100% dimethyl sulfoxide (Sigma), and mice were given sorafenib or vehicle (10 mg/kg) once a day for 16 days by oral gavage. The vehicle solution for sorafenib consisted of 30% (w/v) Cremophor EL, 30% (w/v) PEG-400 (polyethylene glycol, molecular weight 400), 10% ethanol, and 10% glucose (all Sigma-Aldrich). Some mice were also given the combined treatment of sorafenib and IPI-926. The vehicle-treated group received both 5% β-cyclodextrin solution and the vehicle solution for sorafenib.

Antibodies and FACS

Monoclonal antibodies against Mac1, Gr1, B220, and CD3 (all from eBioscience) were used for peripheral blood analysis. Bone marrow lineage staining was carried out with biotinylated antibodies against Gr1, Ter119, B220, and CD3 (all from eBioscience). Bone marrow cells were also stained with antibodies against cKit, Sca1, CD16/32, CD34, FLT3, CD150, CD48, and IL-7R (all from eBioscience). Flow cytometry and BrdU staining were carried out as previously described (69). Apoptosis was determined by Annexin V binding (BD Biosciences). Flow cytometry was performed on FACSCalibur or LSRII flow cytometers (BD Biosciences) and analyzed with FlowJo software. Cell sorting was carried out on a FACSARIA II (BD Biosciences).

Quantitative real-time PCR analysis

Total RNA was extracted with the RNeasy Plus Mini Kit (Qiagen) and reverse-transcribed with SuperScript III reverse transcriptase (Invitrogen). qRT-PCR was carried out with TaqMan and SYBR Green Master Mix (ABI) according to the manufacturer's protocols (table S2).

Microarray and GSEA analysis

Analysis of published data sets (3, 26, 27) involved normalized gene expression data, as originally provided by the authors, downloaded from the National Center for Biotechnology Information Gene Expression Omnibus (GEO) database (GSE10358, GSE14468), the TCGA Research Network (AML) at <http://cancergenome.nih.gov>, or cBioPortal at <http://www.cbioportal.org/public-portal> (70, 71). Log₂-transformed *GLI2* and *GLL1* gene expression was compared between *FLT3*-ITD and wild-type *FLT3* tumors using *t* test. KSL and GMP cells were isolated by FACS from wild-type, *Flt3*/ITD, and *Flt3*/ITD-*SmoM2* animals

RESEARCH ARTICLE

at about 3 months of age or when Flt3/ITD-SmoM2 animals were moribund. Total RNA was extracted and hybridized onto the Affymetrix Mouse Genome 430 2.0 array (Affymetrix) followed by microarray scanning with the Affymetrix GeneChip scanner and data analysis with the GeneChip Operating Software (Affymetrix). Gene expression data preprocessing and normalization were performed by the frozen robust multiarray analysis (fRMA) method (72). Gene set enrichment analysis was performed with JAVA-based GSEA software provided by the Broad Institute of the Massachusetts Institute of Technology (39). The AFA was performed as previously described (40, 41). Gene sets were obtained from Molecular Signatures Database (MSigDB, C2 collection). Antiapoptosis gene set was obtained from the Gene Ontology collection (GO:0006916). The curated gene set of STAT5 signature in CD34⁺ HSPCs was obtained from MSigDB and was previously published (73).

Western blot

Cell lysates were separated by SDS-polyacrylamide gel electrophoresis followed by Western blotting using rabbit anti-total STAT5 (#9396), pSTAT5-Y694 (#9351), total STAT3 (#12640), total AKT (#9272), pAKT (#9271), total ERK1/2 (#9102), and pERK (#9101), all from Cell Signaling, or tubulin (#21058; Abcam), followed by a horseradish peroxidase-conjugated goat anti-rabbit secondary antibody (#NA934V; Amersham). Film was developed using Amersham ECL Plus Western Blotting Detection Reagents (GE Healthcare). Images were obtained with the GS-900 calibrated densitometer and quantified with Image Lab software (Bio-Rad).

Small interfering RNA

MV4-11 and Molm-14 cell lines were transfected with ON-TARGETplus SMARTpool siRNAs targeting human *SMO* and *GLI2* (Dharmacon), using an Amaxa Nucleofector (Lonza). Successful knockdown of the genes was determined by qRT-PCR 24 hours after transfection, after which cells were treated with sorafenib.

Statistics

Log-rank (Mantel-Cox) test *P* values for the Kaplan-Meier survival curves were generated using GraphPad Prism. All other *P* values were calculated with unpaired two-tailed Student's *t* test, unless otherwise specified. All experiments were performed independently at least three times. Pearson's *R* value for correlation and *P* value was generated in GraphPad Prism. *P* values <0.05 were considered statistically significant. Original data for patient samples and animal experiments are provided in table S3.

SUPPLEMENTARY MATERIALS

www.sciencetranslationalmedicine.org/cgi/content/full/7/291/291ra96/DC1

Fig. S1. GLI2 is expressed in FLT3-ITD AML clinical specimens.

Fig. S2. Flt3/ITD-SmoM2 transgenic mice express Hh pathway genes and develop clinically relevant AML.

Fig. S3. Specific bone marrow hematopoietic stem cell and myeloid progenitor compartments are maintained in Flt3/ITD-SmoM2 mice.

Fig. S4. Leukemia formation in Flt3/ITD-SmoM2 mice is cell-intrinsic.

Fig. S5. GSEA reveals increased STAT5 signaling in Flt3/ITD and antiapoptotic features in Flt3/ITD-SmoM2 mice.

Fig. S6. The combination of sorafenib and IPI-926 limits the growth of FLT3-ITD AML.

Fig. S7. Hh signaling affects FLT3-ITD at the level of STAT5.

Fig. S8. IPI-926 inhibits the expression of Hh target genes in Flt3/ITD-SmoM2 bone marrow cells.

Table S1. Leukemic organ infiltration.

Table S2. PCR primers.

Table S3. Original data (provided as a separate Excel file).

REFERENCES AND NOTES

1. S. Fröhling, R. F. Schlenk, J. Breitnick, A. Benner, S. Kreitmeier, K. Tobis, H. Döhner, K. Dohner, AML Study Group Ulm, Prognostic significance of activating *FLT3* mutations in younger adults (16 to 60 years) with acute myeloid leukemia and normal cytogenetics: A study of the AML Study Group Ulm. *Blood* **100**, 4372–4380 (2002).
2. J. P. Patel, M. Gönen, M. E. Figueroa, H. Fernandez, Z. Sun, J. Racevskis, P. Van Vlierberghe, I. Dolgalev, S. Thomas, O. Aminova, K. Huberman, J. Cheng, A. Viale, N. D. Socci, A. Heguy, A. Chery, G. Vance, R. R. Higgins, R. P. Ketterling, R. E. Gallagher, M. Litow, M. R. M. van den Brink, H. M. Lazarus, J. M. Rowe, S. Luger, A. Ferrando, E. Paietta, M. S. Tallman, A. Melnick, O. Abdel-Wahab, R. L. Levine, Prognostic relevance of integrated genetic profiling in acute myeloid leukemia. *N. Engl. J. Med.* **366**, 1079–1089 (2012).
3. Cancer Genome Atlas Research Network, Genomic and epigenomic landscapes of adult de novo acute myeloid leukemia. *N. Engl. J. Med.* **368**, 2059–2074 (2013).
4. M. C. Stubbs, Y. M. Kim, A. V. Krivtsov, R. D. Wright, Z. Feng, J. Agarwal, A. L. Kung, S. A. Armstrong, MLL-AF9 and FLT3 cooperation in acute myelogenous leukemia: Development of a model for rapid therapeutic assessment. *Leukemia* **22**, 66–77 (2008).
5. H. G. Kim, K. Kojima, C. S. Swindle, C. V. Cotta, Y. Huo, V. Reddy, C. A. Klug, FLT3-ITD cooperates with inv(16) to promote progression to acute myeloid leukemia. *Blood* **111**, 1567–1574 (2008).
6. N. A. Zorko, K. M. Bemot, S. P. Whitman, R. F. Siebenaler, E. H. Ahmed, G. G. Marcucci, D. A. Yanes, K. K. McConnell, C. Mao, C. Kalu, X. Zhang, D. Jarjoura, A. M. Dorrance, N. A. Heerema, B. H. Lee, G. Huang, G. Marcucci, M. A. Caligiuri, MLL partial tandem duplication and *Flt3* internal tandem duplication in a double knock-in mouse recapitulates features of counterpart human acute myeloid leukemias. *Blood* **120**, 1130–1136 (2012).
7. S. Greenblatt, L. Li, C. Slape, B. Nguyen, R. Novak, A. Duffield, D. Huso, S. Desiderio, M. J. Borowitz, P. Aplan, D. Small, Knock-in of a FLT3/ITD mutation cooperates with a NUP98-HOXD13 fusion to generate acute myeloid leukemia in a mouse model. *Blood* **119**, 2883–2894 (2012).
8. K. Reckzeh, O. Bereshchenko, A. Mead, M. Rehn, S. Kharazi, S. E. Jacobsen, C. Nerlov, J. Cammenga, Molecular and cellular effects of oncogene cooperation in a genetically accurate AML mouse model. *Leukemia* **26**, 1527–1536 (2012).
9. M. Mallardo, A. Caronno, G. Pruneri, P. R. Raviele, A. Viale, P. G. Pelicci, E. Colombo, NPMc+ and FLT3-ITD mutations cooperate in inducing acute leukaemia in a novel mouse model. *Leukemia* **27**, 2248–2251 (2013).
10. R. Rau, D. Magoon, S. Greenblatt, L. Li, C. Annesley, A. S. Duffield, D. Huso, E. McIntyre, J. G. Clohessy, M. Reschke, P. P. Pandolfi, D. Small, P. Brown, NPMc+ cooperates with Flt3/ITD mutations to cause acute leukemia recapitulating human disease. *Exp. Hematol.* **42**, 101–113.e5 (2014).
11. L. M. Kats, M. Reschke, R. Taulli, O. Pozdnyakova, K. Burgess, P. Bhargava, K. Straley, R. Karnik, A. Meissner, D. Small, S. M. Su, K. Yen, J. Zhang, P. P. Pandolfi, Proto-oncogenic role of mutant *IDH2* in leukemia initiation and maintenance. *Cell Stem Cell* **14**, 329–341 (2014).
12. R. McMillan, W. Matsui, Molecular pathways: The Hedgehog signaling pathway in cancer. *Clin. Cancer Res.* **18**, 4883–4888 (2012).
13. D. D. Von Hoff, P. M. Lorusso, C. M. Rudin, J. C. Reddy, R. L. Yauch, R. Tibes, G. J. Weiss, M. J. Borad, C. L. Hann, J. R. Brahmer, H. M. Mackey, B. L. Lum, W. C. Darbonne, J. C. Marsters Jr., F. J. de Sauvage, J. A. Low, Inhibition of the hedgehog pathway in advanced basal-cell carcinoma. *N. Engl. J. Med.* **361**, 1164–1172 (2009).
14. C. D. Peacock, Q. Wang, G. S. Gesell, I. M. Corcoran-Schwartz, E. Jones, J. Kim, W. L. Devereux, J. T. Rhodes, C. A. Huff, P. A. Beachy, D. N. Watkins, W. Matsui, Hedgehog signaling maintains a tumor stem cell compartment in multiple myeloma. *Proc. Natl. Acad. Sci. U.S.A.* **104**, 4048–4053 (2007).
15. T. L. Lin, Q. H. Wang, P. Brown, C. Peacock, A. A. Merchant, S. Brennan, E. Jones, K. McGovern, D. N. Watkins, K. M. Sakamoto, W. Matsui, Self-renewal of acute lymphocytic leukemia cells is limited by the Hedgehog pathway inhibitors cyclopamine and IPI-926. *PLOS One* **5**, e15262 (2010).
16. C. Dierks, R. Beigi, G.-R. Guo, K. Zirlik, M. R. Stegert, P. Manley, C. Trussell, A. Schmitt-Graeff, K. Landwerlin, H. Veelken, M. Warmuth, Expansion of Bcr-Abl-positive leukemic stem cells is dependent on Hedgehog pathway activation. *Cancer Cell* **14**, 238–249 (2008).
17. C. Zhao, A. Chen, C. H. Jamieson, M. Fereshteh, A. Abrahamsson, J. Blum, H. Y. Kwon, J. Kim, J. P. Chute, D. Rizzieri, M. Munchhof, T. VanArsdale, P. A. Beachy, T. Reya, Hedgehog signalling is essential for maintenance of cancer stem cells in myeloid leukaemia. *Nature* **458**, 776–779 (2009).
18. I. Hofmann, E. H. Stover, D. E. Cullen, J. Mao, K. J. Morgan, B. H. Lee, M. G. Kharas, P. G. Miller, M. G. Comejo, R. Okabe, S. A. Armstrong, N. Ghilardi, S. Gould, F. J. de Sauvage, A. P. McMahon, D. G. Gilliland, Hedgehog signaling is dispensable for adult murine hematopoietic stem cell function and hematopoiesis. *Cell Stem Cell* **4**, 559–567 (2009).

19. N. Kessar, F. Jamen, L. L. Rubin, W. D. Richardson, Cooperation between sonic hedgehog and fibroblast growth factor/MAPK signalling pathways in neocortical precursors. *Development* **131**, 1289–1298 (2004).
20. F. Götschel, D. Berg, W. Gruber, C. Bender, M. Eberl, M. Friedel, J. Sonntag, E. Rüngeler, H. Hache, C. Wierling, W. Nietfeld, H. Lehrach, A. Frischauf, R. Schwartz-Albiez, F. Aberger, U. Korf, Synergism between Hedgehog-Gli and EGFR signaling in Hedgehog-responsive human medulloblastoma cells induces downregulation of canonical Hedgehog-target genes and stabilized expression of GLI1. *PLOS One* **8**, e65403 (2013).
21. H. Schnidar, M. Eberl, S. Klingler, D. Mangelberger, M. Kasper, C. Hauser-Kronberger, G. Regl, R. Kroismayr, R. Morigg, M. Sibilia, F. Aberger, Epidermal growth factor receptor signaling synergizes with Hedgehog/Gli in oncogenic transformation via activation of the MEK/ERK/JUN pathway. *Cancer Res* **69**, 1284–1292 (2009).
22. P. J. M. Valk, R. G. W. Verhaak, M. A. Beijten, C. A. J. Erpelinck, S. B. v. W. van Doorn-Khosrovani, J. M. Boer, H. B. Beverloo, M. J. Moorhouse, P. J. van der Spek, B. Löwenberg, R. Delwel, Prognostically useful gene-expression profiles in acute myeloid leukemia. *N. Engl. J. Med.* **350**, 1617–1628 (2004).
23. C. B. Bai, W. Auerbach, J. S. Lee, D. Stephen, A. L. Joyner, *Gli2*, but not *Gli1*, is required for initial Shh signaling and ectopic activation of the Shh pathway. *Development* **129**, 4753–4761 (2002).
24. J. Kim, M. Kato, P. A. Beachy, Gli2 trafficking links Hedgehog-dependent activation of Smoothened in the primary cilium to transcriptional activation in the nucleus. *Proc. Natl. Acad. Sci. U.S.A.* **106**, 21666–21671 (2009).
25. G. Regl, G. W. Neill, T. Eichberger, M. Kasper, M. S. Ikram, J. Koller, H. Hintner, A. G. Quinn, A.-M. Frischauf, F. Aberger, Human GLI2 and GLI1 are part of a positive feedback mechanism in basal cell carcinoma. *Oncogene* **21**, 5529–5539 (2002).
26. M. H. Tomasson, Z. Xiang, R. Walgren, Y. Zhao, Y. Kasai, T. Miner, R. E. Ries, O. Lubman, D. H. Fremont, M. D. McLellan, J. E. Payton, P. Westervelt, J. F. DiPersio, D. C. Link, M. J. Walter, T. A. Graubert, M. Watson, J. Baty, S. Heath, W. D. Shannon, R. Nagarajan, C. D. Bloomfield, E. R. Mardis, R. K. Wilson, T. J. Ley, Somatic mutations and germline sequence variants in the expressed tyrosine kinase genes of patients with de novo acute myeloid leukemia. *Blood* **111**, 4797–4808 (2008).
27. E. Taskesen, L. Bullinger, A. Corbacioglu, M. A. Sanders, C. A. Erpelinck, B. J. Wouters, S. C. van der Poel-van Luytgaard, F. Damm, J. Krauter, A. Ganser, R. F. Schlenk, B. Löwenberg, R. Delwel, H. Döhner, P. J. Valk, K. Döhner, Prognostic impact, concurrent genetic mutations, and gene expression features of AML with *CEBPA* mutations in a cohort of 1182 cytogenetically normal AML patients: Further evidence for *CEBPA* double mutant AML as a distinctive disease entity. *Blood* **117**, 2469–2475 (2011).
28. L. Li, O. Piloto, H. B. Nguyen, K. Greenberg, K. Takamiya, F. Racke, D. Huso, D. Small, Knock-in of an internal tandem duplication mutation into murine FLT3 confers myeloproliferative disease in a mouse model. *Blood* **111**, 3849–3858 (2008).
29. J. Mao, K. L. Ligon, E. Y. Rakhlin, S. P. Thayer, R. T. Bronson, D. Rowitch, A. P. McMahon, A novel somatic mouse model to survey tumorigenic potential applied to the Hedgehog pathway. *Cancer Res* **66**, 10171–10178 (2006).
30. R. Kühn, F. Schwenk, M. Aguet, K. Rajewsky, Inducible gene targeting in mice. *Science* **269**, 1427–1429 (1995).
31. Q. Ding, J. Motoyama, S. Gasca, R. Mo, H. Sasaki, J. Rossant, C. C. Hui, Diminished Sonic hedgehog signaling and lack of floor plate differentiation in *Gli2* mutant mice. *Development* **125**, 2533–2543 (1998).
32. S. Miyagawa, D. Matsumaru, A. Murashima, A. Omori, Y. Satoh, R. Haraguchi, J. Motoyama, T. Iguchi, N. Nakagata, C.-c. Hui, G. Yamada, The role of Sonic hedgehog-Gli2 pathway in the masculinization of external genitalia. *Endocrinology* **152**, 2894–2903 (2011).
33. S. C. Kogan, J. M. Ward, M. R. Anver, J. J. Berman, C. Brayton, R. D. Cardiff, J. S. Carter, S. de Coronado, J. R. Downing, T. N. Fredrickson, D. C. Haines, A. W. Harris, N. L. Harris, H. Hiai, E. S. Jaffe, I. C. MacLennan, P. P. Pandolfi, P. K. Pattengale, A. S. Perkins, R. M. Simpson, M. S. Tuttle, J. F. Wong, H. C. Morse III; Hematopathology subcommittee of the Mouse Models of Human Cancers Consortium, Bethesda proposals for classification of nonlymphoid hematopoietic neoplasms in mice. *Blood* **100**, 238–245 (2002).
34. D. G. Gilliland, J. D. Griffin, The roles of FLT3 in hematopoiesis and leukemia. *Blood* **100**, 1532–1542 (2002).
35. F. Varnat, A. Duquet, M. Malerba, M. Zbinden, C. Mas, P. Gervaz, A. Ruiz i Altaba, Human colon cancer epithelial cells harbour active HEDGEHOG-Gli signaling that is essential for tumour growth, recurrence, metastasis and stem cell survival and expansion. *EMBO Mol. Med.* **1**, 338–351 (2009).
36. K.-S. Park, L. G. Martelotto, M. Peifer, M. L. Sos, A. N. Karnezis, M. R. Mahjoub, K. Bernard, J. F. Conklin, A. Szczepny, J. Yuan, R. Guo, B. Ospina, J. Falzon, S. Bennett, T. J. Brown, A. Markovic, W. L. Devereux, C. A. Ocasio, J. K. Chen, T. Stearns, R. K. Thomas, M. Dorsch, S. Buonamici, D. N. Watkins, C. D. Peacock, J. Sage, A crucial requirement for Hedgehog signaling in small cell lung cancer. *Nat. Med.* **17**, 1504–1508 (2011).
37. R. L. Yauch, S. E. Gould, S. J. Scales, T. Tang, H. Tian, C. P. Ahn, D. Marshall, L. Fu, T. Januario, D. Kallop, M. Nannini-Pepe, K. Kotkow, J. C. Marsters, L. L. Rubin, F. J. de Sauvage, A paracrine requirement for hedgehog signalling in cancer. *Nature* **455**, 406–410 (2008).
38. S. H. Chu, D. Heiser, L. Li, I. Kaplan, M. Collector, D. Huso, S. J. Sharkis, C. Civin, D. Small, FLT3-ITD knockin impairs hematopoietic stem cell quiescence/homeostasis, leading to myelo-proliferative neoplasm. *Cell Stem Cell* **11**, 346–358 (2012).
39. A. Subramanian, P. Tamayo, V. K. Mootha, S. Mukherjee, B. L. Ebert, M. A. Gillette, A. Paulovich, S. L. Pomeroy, T. R. Golub, E. S. Lander, J. P. Mesirov, Gene set enrichment analysis: A knowledge-based approach for interpreting genome-wide expression profiles. *Proc. Natl. Acad. Sci. U.S.A.* **102**, 15545–15550 (2005).
40. M. S. Kortenhorst, M. D. Wissing, R. Rodríguez, S. K. Kachhap, J. J. Jans, P. Van der Groep, H. M. Verheul, A. Gupta, P. O. Aiyetan, E. van der Wall, M. A. Carducci, P. J. Van Diest, L. Marchionni, Analysis of the genomic response of human prostate cancer cells to histone deacetylase inhibitors. *Epigenetics* **8**, 907–920 (2013).
41. A. E. Ross, L. Marchionni, M. Vuica-Ross, C. Cheadle, J. Fan, D. M. Berman, E. M. Schaeffer, Gene expression pathways of high grade localized prostate cancer. *Prostate* **71**, 1568–1577 (2011).
42. L. Li, E. Bailey, S. Greenblatt, D. Huso, D. Small, Loss of the wild-type allele contributes to myeloid expansion and disease aggressiveness in FLT3/ITD knockin mice. *Blood* **118**, 4935–4945 (2011).
43. S. Kharazi, A. J. Mead, A. Mansour, A. Hultquist, C. Böiers, S. Luc, N. Buza-Vidas, Z. Ma, H. Ferry, D. Atkinson, K. Reckzeh, K. Masson, J. Cammenga, L. Rönstrand, F. Arai, T. Suda, C. Nerlov, E. Sitnicka, S. E. Jachosni, M. Vuica-Ross, C. Cheadle, J. Fan, D. M. Berman, E. M. Schaeffer, *Flt3-ITD*-induced myeloproliferation. *Blood* **118**, 3613–3621 (2011).
44. B. D. Smith, M. Levis, M. Beran, F. Giles, H. Kantarjian, K. Berg, K. M. Murphy, T. Dausies, J. Allebach, D. Small, Single-agent CEP-701, a novel FLT3 inhibitor, shows biologic and clinical activity in patients with relapsed or refractory acute myeloid leukemia. *Blood* **103**, 3669–3676 (2004).
45. R. M. Stone, D. J. DeAngelo, V. Klimek, I. Galinsky, E. Estey, S. D. Nimer, W. Grandin, D. Lebowitz, Y. Wang, P. Cohen, E. A. Fox, D. Neuberger, J. Clark, D. G. Gilliland, J. D. Griffin, Patients with acute myeloid leukemia and an activating mutation in FLT3 respond to a small-molecule FLT3 tyrosine kinase inhibitor, PKC412. *Blood* **105**, 54–60 (2005).
46. S. Knapper, A. K. Burnett, T. Littlewood, W. J. Kell, S. Agrawal, R. Chopra, R. Clark, M. J. Levis, D. Small, A phase 2 trial of the FLT3 inhibitor lestauritinib (CEP701) as first-line treatment for older patients with acute myeloid leukemia not considered fit for intensive chemotherapy. *Blood* **108**, 3262–3270 (2006).
47. T. Fischer, R. M. Stone, D. J. DeAngelo, I. Galinsky, E. Estey, C. Lanza, E. Fox, G. Ehninger, E. J. Feldman, G. J. Schiller, V. M. Klimek, S. D. Nimer, D. G. Gilliland, C. Dutreix, A. Huntsman-Labeled, J. Virkus, F. J. Giles, Phase IIB trial of oral midostaurin (PKC412), the FMS-like tyrosine kinase 3 receptor (FLT3) and multi-targeted kinase inhibitor, in patients with acute myeloid leukemia and high-risk myelodysplastic syndrome with either wild-type or mutated FLT3. *J. Clin. Oncol.* **28**, 4339–4345 (2010).
48. D. Small, Targeting FLT3 for the treatment of leukemia. *Semin. Hematol.* **45**, S17–S21 (2008).
49. Y. Matsuo, R. MacLeod, C. Uphoff, H. Drexler, C. Nishizaki, Y. Katayama, G. Kimura, N. Fujii, E. Omoto, M. Harada, K. Orita, Two acute monocytic leukemia (AML-M5a) cell lines (MOLM-13 and MOLM-14) with interclonal phenotypic heterogeneity showing MLL-AF9 fusion resulting from an occult chromosome insertion, ins (11; 9)(q23; p22p23). *Leukemia* **11**, 1469–1477 (1997).
50. W. Zhang, M. Konopleva, Y. X. Shi, T. McQueen, D. Harris, X. Ling, Z. Estrov, A. Quintás-Cardama, D. Small, J. Cortes, M. Andreeff, Mutant FLT3: A direct target of sorafenib in acute myelogenous leukemia. *J. Natl. Cancer Inst.* **100**, 184–198 (2008).
51. M. R. Tremblay, A. Lescarbeau, M. J. Grogan, E. Tan, G. Lin, B. C. Austad, L. C. Yu, M. L. Behnke, S. J. Nair, M. Hagel, K. White, J. Conley, J. D. Manna, T. M. Alvarez-Diez, J. Hoyt, C. N. Woodward, J. R. Sydor, M. Pink, J. MacDougall, M. J. Campbell, J. Cushing, J. Ferguson, M. S. Curtis, K. McGovern, M. A. Read, V. J. Palombella, J. Adams, A. C. Castro, Discovery of a potent and orally active hedgehog pathway antagonist (IPI-926). *J. Med. Chem.* **52**, 4400–4418 (2009).
52. D. Auclair, D. Miller, V. Yatsula, W. Pickett, C. Carter, Y. Chang, X. Zhang, D. Wilkie, A. Burd, H. Shi, S. Rocks, R. Gedrich, L. Abriola, H. Vasavada, M. Lynch, J. Dumas, P. A. Trail, S. M. Wilhelm, Antitumor activity of sorafenib in FLT3-driven leukemic cells. *Leukemia* **21**, 439–445 (2007).
53. K. Tse, J. Allebach, M. Levis, B. Smith, F. Bohmer, D. Small, Inhibition of the transforming activity of FLT3 internal tandem duplication mutants from AML patients by a tyrosine kinase inhibitor. *Leukemia* **16**, 2027–2036 (2002).
54. A. Puissant, N. Fenouille, G. Alexe, Y. Pikman, C. F. Bassil, S. Mehta, J. Du, J. U. Kazi, F. Luciano, L. Rönstrand, A. L. Kung, J. C. Aster, I. Galinsky, R. M. Stone, D. J. DeAngelo, M. T. Hemann, K. Stegmaier, SYK is a critical regulator of FLT3 in acute myeloid leukemia. *Cancer Cell* **25**, 226–242 (2014).
55. M. Levis, FLT3 mutations in acute myeloid leukemia: What is the best approach in 2013? *Hematology Am. Soc. Hematol. Educ. Program* **2013**, 220–226 (2013).
56. S. Wilhelm, C. Carter, M. Lynch, T. Lowinger, J. Dumas, R. A. Smith, B. Schwartz, R. Simantov, S. Kelley, Discovery and development of sorafenib: A multikinase inhibitor for treating cancer. *Nat. Rev. Drug Discov.* **5**, 835–844 (2006).
57. O. Nolan-Stevaux, J. Lau, M. L. Truitt, G. C. Chu, M. Hebrok, M. E. Fernández-Zapico, D. Hanahan, *Gli1* is regulated through Smoothened-independent mechanisms in neoplastic pancreatic ducts and mediates PDAC cell survival and transformation. *Genes Dev.* **23**, 24–36 (2009).
58. F. Aberger, A. Ruiz i Altaba, Context-dependent signal integration by the Gli code: The oncogenic load, pathways, modifiers and implications for cancer therapy. *Semin. Cell Dev. Biol.* **33**, 93–104 (2014).

59. B. Stecca, C. Mas, V. Clement, M. Zbinden, R. Correa, V. Piguet, F. Beermann, A. Ruiz i Altaba, Melanomas require HEDGEHOG-GLI signaling regulated by interactions between GLI1 and the RAS-MEK/AKT pathways. *Proc. Natl. Acad. Sci. U.S.A.* **104**, 5895–5900 (2007).
60. K. F. Tse, G. Mukherjee, D. Small, Constitutive activation of FLT3 stimulates multiple intracellular signal transducers and results in transformation. *Leukemia* **14**, 1766–1776 (2000).
61. A. Brady, S. Gibson, L. Rybicki, E. Hsi, Y. Saunthararajah, M. A. Sekeres, R. Tiu, E. Copelan, M. Kalaycio, R. Sobecks, J. Bates, A. S. Advani, Expression of phosphorylated signal transducer and activator of transcription 5 is associated with an increased risk of death in acute myeloid leukemia. *Eur. J. Haematol.* **89**, 288–293 (2012).
62. M. Fiaschi, B. Rozell, A. Bergström, R. Toftgård, M. I. Kleman, Targeted expression of GLI1 in the mammary gland disrupts pregnancy-induced maturation and causes lactation failure. *J. Biol. Chem.* **282**, 36090–36101 (2007).
63. J. Wang, N. Pham-Mitchell, C. Schindler, I. L. Campbell, Dysregulated Sonic hedgehog signaling and medulloblastoma consequent to IFN- α -stimulated STAT2-independent production of IFN- γ in the brain. *J. Clin. Invest.* **112**, 535–543 (2003).
64. E. Y. Lee, H. Ji, Z. Ouyang, B. Zhou, W. Ma, S. A. Vokes, A. P. McMahon, W. H. Wong, M. P. Scott, Hedgehog pathway-regulated gene networks in cerebellum development and tumorigenesis. *Proc. Natl. Acad. Sci. U.S.A.* **107**, 9736–9741 (2010).
65. R. Moriggl, V. Sexl, L. Kenner, C. Dunsch, K. Stangl, S. Gingras, A. Hoffmeyer, A. Bauer, R. Piekorz, D. Wang, K. D. Bunting, E. F. Wagner, K. Sonneck, P. Valent, J. N. Ihle, H. Beug, Stat5 tetramer formation is associated with leukemogenesis. *Cancer Cell* **7**, 87–99 (2005).
66. A. Hoelbl, C. Schuster, B. Kovacic, B. Zhu, M. Wickre, M. A. Hoelzl, S. Fajmann, F. Grebien, W. Warsch, G. Stengl, L. Hennighausen, V. Poli, H. Beug, R. Moriggl, V. Sexl, Stat5 is indispensable for the maintenance of *bcr/abl*-positive leukaemia. *EMBO Mol. Med.* **2**, 98–110 (2010).
67. K. W. Pratz, J. Cortes, G. J. Roboz, N. Rao, O. Arowojolu, A. Stine, Y. Shiotsu, A. Shudo, S. Akinaga, D. Small, J. E. Karp, M. Levis, A pharmacodynamic study of the FLT3 inhibitor KW-2449 yields insight into the basis for clinical response. *Blood* **113**, 3938–3946 (2009).
68. H. A. Zahreddine, B. Culjkovic-Kraljacic, S. Assouline, P. Gendron, A. A. Romeo, S. J. Morris, G. Cormack, J. B. Jaquith, L. Cerchietti, E. Cocolakis, A. Amri, J. Bergeron, B. Leber, M. W. Becker, S. Pei, C. T. Jordan, W. H. Miller, K. L. Borden, The sonic hedgehog factor GLI1 imparts drug resistance through inducible glucuronidation. *Nature* **511**, 90–93 (2014).
69. A. Merchant, G. Joseph, Q. Wang, S. Brennan, W. Matsui, Gli1 regulates the proliferation and differentiation of HSC and myeloid progenitors. *Blood* **115**, 2391–2396 (2010).
70. E. Cerami, J. Gao, U. Dogrusoz, B. E. Gross, S. O. Sumer, B. A. Aksoy, A. Jacobsen, C. J. Byrne, M. L. Heuer, E. Larsson, Y. Antipin, B. Reva, A. P. Goldberg, C. Sander, N. Schultz, The cBio cancer genomics portal: An open platform for exploring multidimensional cancer genomics data. *Cancer Discov.* **2**, 401–404 (2012).
71. J. Gao, B. A. Aksoy, U. Dogrusoz, G. Dresdner, B. Gross, S. O. Sumer, Y. Sun, A. Jacobsen, R. Sinha, E. Larsson, E. Cerami, C. Sander, N. Schultz, Integrative analysis of complex cancer genomics and clinical profiles using the cBioPortal. *Sci. Signal.* **6**, pii1 (2013).
72. M. N. McCall, B. M. Bolstad, R. A. Irizarry, Frozen robust multiarray analysis (fRMA). *Biostatistics* **11**, 242–253 (2010).
73. A. T. Wierenga, E. Vellenga, J. J. Schuringa, Maximal STAT5-induced proliferation and self-renewal at intermediate STAT5 activity levels. *Mol. Cell Biol.* **28**, 6668–6680 (2008).

Acknowledgments: We thank all patients and donors who contributed peripheral blood and/or bone marrow specimens for these studies. **Funding:** This study was supported by research grants from the NIH (R01CA127574, R01CA174951, R01CA090668, R21CA155733, P30DK090868, P30CA006973, and UL1TR001079) to W.M., D.S., D.L.H., and L.M. Support was also provided by the Leukemia and Lymphoma Society, the Gabrielle's Angel Foundation for Cancer Research, the Edward P. Evans Foundation, and the Petre Foundation. **Author contributions:** Y.L. and W.M. designed the studies, analyzed the data, and wrote the manuscript. Y.L., L.G., LL, Q.W., H.M., E.C., D.L.H., S.F., C.D.P., and A.A.M. carried out the studies. K.M., D.N.W., and A.A.M. contributed to the design and performance of some of the studies. L.G. and L.M. carried out the bioinformatics studies. B.D.S. and M.L. provided the clinical specimens. L.G., B.D.S., A.A.M., and D.S. contributed to the study design and writing of the manuscript. **Competing interests:** K.M. is an employee of Infinity Pharmaceuticals. The other authors declare that they have no competing interests. **Data and materials availability:** Oligonucleotide microarray data have been deposited in the GEO under accession number GSE67134. IPI-926 was obtained from Infinity Pharmaceuticals through a materials transfer agreement with Johns Hopkins University.

Submitted 27 December 2014

Accepted 8 May 2015

Published 10 June 2015

10.1126/scitranslmed.aaa5731

Citation: Y. Lim, L. Gondek, L. Li, Q. Wang, H. Ma, E. Chang, D. L. Huso, S. Foerster, L. Marchionni, K. McGovern, D. N. Watkins, C. D. Peacock, M. Levis, B. D. Smith, A. A. Merchant, D. Small, W. Matsui, Integration of Hedgehog and mutant FLT3 signaling in myeloid leukemia. *Sci. Transl. Med.* **7**, 291ra96 (2015).



Integration of Hedgehog and mutant FLT3 signaling in myeloid leukemia

Yiting Lim, Lukasz Gondek, Li Li, Qiuju Wang, Hayley Ma, Emily Chang, David L. Huso, Sarah Foerster, Luigi Marchionni, Karen McGovern, David Neil Watkins, Craig D. Peacock, Mark Levis, Bruce Douglas Smith, Akil A. Merchant, Donald Small and William Matsui (June 10, 2015)

Science Translational Medicine 7 (291), 291ra96. [doi: 10.1126/scitranslmed.aaa5731]

Editor's Summary

Hedgehog to the rescue

Acute myeloid leukemia is generally difficult to treat, and the presence of internal tandem duplication in a gene called *FLT3* (*FLT3-ITD*) is associated with a particularly poor prognosis. Lim *et al.* discovered that patients with *FLT3-ITD* leukemia also have increased activity of the Hedgehog protein signaling pathway. Experiments in mouse models of *FLT3-ITD* confirmed the functional role of Hedgehog in the development of leukemia and showed that combined treatment targeting *FLT3* and Hedgehog is effective as a therapeutic strategy in this setting.

The following resources related to this article are available online at <http://stm.sciencemag.org>. This information is current as of November 22, 2015.

Article Tools	Visit the online version of this article to access the personalization and article tools: http://stm.sciencemag.org/content/7/291/291ra96
Supplemental Materials	"Supplementary Materials" http://stm.sciencemag.org/content/suppl/2015/06/08/7.291.291ra96.DC1
Related Content	The editors suggest related resources on <i>Science's</i> sites: http://stke.sciencemag.org/content/sigtrans/4/157/ra4.full http://stm.sciencemag.org/content/scitransmed/7/295/295er6.full http://stke.sciencemag.org/content/sigtrans/8/394/ra92.full
Permissions	Obtain information about reproducing this article: http://www.sciencemag.org/about/permissions.dtl

Science Translational Medicine (print ISSN 1946-6234; online ISSN 1946-6242) is published weekly, except the last week in December, by the American Association for the Advancement of Science, 1200 New York Avenue, NW, Washington, DC 20005. Copyright 2015 by the American Association for the Advancement of Science; all rights reserved. The title *Science Translational Medicine* is a registered trademark of AAAS.